Published in final edited form as:
*Clin Nucl Med*. 2013 December ; 38(12): 949–956. doi:10.1097/RLU.0000000000000248.

# $^{99m}$Tc-Sestamibi Using a Direct Conversion Molecular Breast Imaging System to Assess Tumor Response to Neoadjuvant Chemotherapy in Women With Locally Advanced Breast Cancer

**David Mitchell, MB**[*], **Carrie B. Hruska, PhD**[*], **Judy C. Boughey, MD**[†], **Dietlind L. Wahner-Roedler, MD**[‡], **Katie N. Jones, MD**[*], **Cindy Tortorelli, MD**[§], **Amy Lynn Conners, MD**[*], and **Michael K. O'Connor, PhD**[*]

[*]Department of Radiology, Mayo Clinic, Rochester, MN

[†]Department of Surgery, Mayo Clinic, Rochester, MN

[‡]Department of Breast Clinic, Department of Internal Medicine, Mayo Clinic, Rochester, MN

[§]EPIC Imaging Center, Portland, OR

## Abstract

**Purpose—**The objective of this study was to determine the ability of breast imaging with $^{99m}$Tc-sestamibi and a direct conversion–molecular breast imaging (MBI) system to predict early response to neoadjuvant chemotherapy (NAC).

**Methods—**Patients undergoing NAC for breast cancer were imaged with a direct conversion–MBI system before (baseline), at 3 to 5 weeks after onset, and after completion of NAC. Tumor size and tumor-to-background (T/B) uptake ratio measured from MBI images were compared with extent of residual disease at surgery using the residual cancer burden.

**Results—**Nineteen patients completed imaging and proceeded to surgical resection after NAC. Mean reduction in T/B ratio from baseline to 3 to 5 weeks for patients classified as RCB-0 (no residual disease), RCB-1 and RCB-2 combined, and RCB-3 (extensive residual disease) was 56% (SD, 0.20), 28% (SD, 0.20), and 4% (SD, 0.15), respectively. The reduction in the RCB-0 group was significantly greater than in RCB-1/2 ($P$ = 0.036) and RCB-3 ($P$ = 0.001) groups. The area under the receiver operator characteristic curve for determining the presence or absence of residual disease was 0.88. Using a threshold of 50% reduction in T/B ratio at 3 to 5 weeks, MBI predicted presence of residual disease at surgery with a diagnostic accuracy of 89.5% (95% confidence interval [CI], 0.64%–0.99%), sensitivity of 92.3% (95% CI, 0.74%–0.99%), and specificity of 83.3% (95% CI, 0.44%–0.99%). The reduction in tumor size at 3 to 5 weeks was not statistically different between RCB groups.

**Conclusions—**Changes in T/B ratio on MBI images performed at 3 to 5 weeks following initiation of NAC were accurate at predicting the presence or absence of residual disease at NAC completion.

### Keywords

molecular breast imaging; neoadjuvant chemotherapy; $^{99m}$Tc-sestamibi; breast cancer



Reprints: Michael K. O'Connor, PhD, Charlton 1, Mayo Clinic, 200 First St SW, Rochester, MN. mkoconnor@mayo.edu..

For patients with locally advanced breast cancer, neoadjuvant chemotherapy (NAC) is a reasonable alternative to adjuvant chemotherapy and has been shown to increase the rates of breast-conserving surgery[1-3] and decrease the need for complete axillary lymph node dissection.[4-6] Use of NAC offers investigators the ability to rapidly evaluate new therapeutic agents[7] and can help accelerate approval of agents in a cost-effective manner.[8,9]

Early prediction of response to NAC offers a potential opportunity to change treatment strategy in cases of inadequate response. Clinical examination, mammography, and ultrasound provide only a modest correlation between tumor size and response to NAC.[10] Further work is needed to establish the value of MRI for NAC response evaluation, because of heterogeneity in study design of investigations performed thus far.[11] Several studies using FDG-PET have shown a correlation between the SUVmax after 1 or 2 courses of chemotherapy and final pathological response.[12,13] However, as with MRI, differences in study design have made it difficult to clearly define its role in monitoring response to NAC.[14]

An alternative functional imaging method for evaluation of response is the use of single-photon imaging techniques using markers such as $^{99m}$Tc-sestamibi. Early work by Mankoff et al[15] showed that breast tumor uptake of sestamibi using a conventional gamma camera could accurately assess the response to NAC. A subsequent study by Tiling et al[16] concluded that sestamibi may be as useful as FDG-PET for the monitoring of tumor response to NAC. One important limitation in the use of conventional gamma cameras for breast imaging is their inability to be easily positioned close to the breast, resulting in poor spatial resolution and inability to detect small tumors and/or small changes in tumor function. Over the last 15 years, several types of compact gamma camera system have been developed that are more optimal for this task. The first generation of dedicated systems utilized a pixelated array of sodium iodide, or cesium iodide crystals, in a small detector and was known as breast-specific gamma imaging (BSGI) systems.[17] In the last 5 years, a new generation of dual detector compact gamma cameras has become commercially available. These systems perform a direct conversion (DC) (nonscintillating) of gamma ray energy to electronic signal using semiconductor detectors and yield improved spatial and energy resolution compared with BSGI systems.[18,19] An additional advantage is that these systems require administered doses of $^{99m}$Tc-sestamibi that are 2 to 3 times lower than those required by the older BSGI systems.[17,20]

In this preliminary study, we investigated the application of a DC–molecular breast imaging (MBI) system and $^{99m}$Tc-sestamibi to evaluate tumor response to NAC. We determined whether changes in tumor uptake of $^{99m}$Tc-sestamibi on MBI performed at 3 to 5 weeks after onset of NAC could predict final pathological tumor response in women with breast cancer.

## PATIENTS AND MATERIALS

### Patient Eligibility and Enrollment

This was a prospective study of patients with newly diagnosed biopsy-proven breast cancer in whom NAC was planned. Women who were pregnant or lactating were excluded. Written informed consent was obtained from all participants as part of an institutional review board–approved protocol.

### Study Design

Each participant underwent 3 MBI studies: a baseline study before initiation of NAC, a second study at 3 to 5 weeks after initiation of NAC, and a third study after completion of

NAC but before surgical resection. The treating oncologist determined the chemotherapy regimen for each patient, and the primary team managed all other aspects of patient care.

### Direct Conversion Molecular Breast Imaging

All imaging studies were performed on 1 of 2 DC-MBI imaging systems: the LumaGem 3200s system (Gamma Medica, Northridge, Calif) or the Discovery NM 750b system (General Electric Medical Systems, Haifa, Israel). Both systems have been described previously in detail and comprise dual-head semiconductor-based detectors[21,22] that allow the breast to be imaged in orientations comparable to mammography. Both systems have been previously shown to have comparable image quality[21] and have been used interchangeable in our laboratory over the last 5 years. To ensure more accurate quantitative analysis, all imaging studies in a given patient were always performed on the same DC-MBI system.

All image acquisitions commenced ~5 minutes after intravenous injection of 300 MBq (8 mCi) $^{99m}$Tc-sestamibi. $^{99m}$Tc-sestamibi has a propensity to adhere to the plastic walls of some types of syringes, and up to 30% residual activity can remain in the syringe.[23] In our laboratory, average residual activity in the injection syringes is 20%. Hence, average administered dose was estimated to be 240 MBq (6.5 mCi), giving an effective radiation dose to the body of 1.9 mSv. Bilateral craniocaudal (CC) and mediolateral oblique (MLO) views were obtained for 10 minutes per view. Molecular breast imaging studies were first interpreted in the course of routine clinical practice by radiologists specializing in breast imaging and according to a validated MBI lexicon.[24]

### Assessment of Tumor Response Using MBI

Following completion of all imaging studies, the MBI images acquired at baseline, 3 to 5 weeks, and at completion of NAC were analyzed by a single breast radiologist (K.N.J.) blinded to patient identity, results from any other imaging modality, and final pathology results that indicated residual disease status. The location of the index tumor was identified in each image. The radiologist measured index tumor size in both views (CC and MLO), and its longest dimension on either view was considered tumor extent.

Quantitative assessment of $^{99m}$Tc-sestamibi uptake was performed using region of interest (ROI) analysis. The MBI image of the breast (CC or MLO), which best demonstrated the greatest extent of the index tumor, was selected for analysis. A tumor ROI was defined to include all pixels with intensities greater than 50% of maximum tumor intensity. An adjacent area of normal breast tissue was selected to represent background activity. The background ROI was placed in an area that was the same distance from the chest wall as the tumor to minimize variance in uptake related to scattered counts from uptake in organs in the chest (eg, heart, liver). If the breast exhibited diffuse tumor uptake suggestive of multifocal or multicentric disease, then the background ROI was placed within normal breast tissue of the contralateral breast.

The tumor-to-background (T/B) ratio was calculated from (mean counts per pixel in the tumor ROI)/(mean counts per pixel in the background ROI). The percentage change in T/B ratio from baseline to 3 to 5 weeks and baseline to post-NAC was calculated.

### Assessment of Pathological Tumor Response

The reference standard for determining residual disease status was pathological examination of resected surgical specimens, specifically evidence of residual invasive disease or carcinoma in situ. Per routine clinical practice, pathology slides were reviewed and reported with particular reference to bidimensional tumor bed area, overall cancer cellularity,

percentage of in situ disease, number of positive lymph nodes, and diameter of largest tumor mass.

If residual invasive disease was present, tumor extent was measured as the longest dimension of contiguous tumor cells. If only microscopic foci of invasive disease were seen, the longest dimension of the fibrotic bed or distribution of tumor cells was measured. Pathological complete response (pCR) was defined as the absence of invasive disease in the breast, with or without the presence of ductal carcinoma in situ (DCIS).

The MD Anderson Residual Cancer Burden Calculator,[25] which incorporates pathological tumor size, overall cancer cellularity, and lymph node status to estimate residual cancer burden (RCB), was used to categorize cancer burden. This is a continuous scale that can be further categorized into the following classes: RCB-0 (no residual disease in breast or in lymph nodes), RCB-1 (minimal residual disease), RCB-2 (moderate residual disease), or RCB-3 (extensive residual disease). Because of the small number of patients in this study, we combined data from classes 1 and 2 to give 3 classes: no residual disease (RCB-0), minimal/moderate residual disease (RCB-1/2), and extensive residual disease (RCB-3).

### Assessment of Tumor Response Using Clinical Assessment and Other Imaging Modalities

Measurements of tumor size from physician-performed clinical examination at the time of each MBI study were abstracted from medical records; the largest dimension was recorded for each examination. Clinical response groupings were defined according to Response Evaluation Criteria In Solid Tumors (RECIST).[26] Radiological measurements of tumor size on mammography and ultrasound were obtained from imaging reports, where available, as the greatest extent of the index tumor measured in any dimension.

### Statistical Analysis

The mean T/B ratio at each time point and the mean percentage reduction in T/B ratio from baseline at 3 to 5 weeks and post-NAC were calculated and compared between each of the partial/nonresponder groups (RCB-1/2 and RCB-3) with the complete-responder group (RCB-0) using the Tukey-Kramer method and analysis of variance for data analysis. A similar analysis was performed on results for tumor size. Ninety-five percent confidence intervals (CIs) and 2-sided $P$ values were reported, where $P < 0.05$ was considered to indicate statistical significance.

To evaluate the ability of a change in T/B ratio from baseline to 3 to 5 weeks to discriminate between RCB-1/2/3 and RCB-0 at completion of NAC, receiver operator characteristic (ROC) analysis was performed using the sensitivity and specificity obtained as a function of a threshold for percent reduction in T/B ratio. The area under the ROC curve (AUC) was calculated as an overall measure of the predictive power for MBI. A similar analysis was then performed for T/B ratio percent reduction from baseline to post-NAC. The optimal threshold that gave the highest accuracy in discriminating between the RCB-1/2/3 and RCB-0 groups was determined. The sensitivity and specificity at this threshold were calculated for the 3-to 5-week MBI and post-NAC MBI.

Pathological tumor size at surgery was compared with post-NAC tumor size on MBI, mammography, ultrasound, and clinical examination, and correlation coefficients were calculated. Fisher r-to-z transformation was used to compare correlation coefficients.

# RESULTS

## Patients

Twenty patients who planned to undergo NAC treatment for breast cancer were prospectively enrolled. One patient voluntarily dropped out and was excluded from further analysis. The remaining 19 patients completed all 3 MBI studies and NAC and underwent surgical resection to negative margins. Patient characteristics are shown in Table 1.

## Pathological Outcomes

At surgery, 8 (42%) of 19 patients had pCR. Of these 8 patients, 3 had residual DCIS with pathological extent of 1.2 and 0.9 cm and microscopic disease.

Eleven (58%) of 19 patients had pathological evidence of residual invasive disease. Six patients had invasive foci of more than 1 cm in extent, 3 patients had subcentimeter foci of invasive disease, and 2 patients had microscopic foci of invasive disease distributed sparsely over fibrotic tumor beds measuring 4.8 and 1.1 cm.

Six patients were classified as RCB-0, one of whom had subcentimeter DCIS at surgery. The discrepancy in the number of patients with RCB-0 (6 patients) and pCR (8 patients) is due to 2 patients with no residual disease in the breast (pCR) but positive lymph nodes (not RCB-0).

Three patients were classified as RCB-1, comprising 1 patient with a single focus of 0.5-cm invasive disease, 1 patient with microscopic DCIS and positive lymph node, and 1 patient with microscopic invasive disease over an 11-cm fibrotic bed. Five patients were classified as RCB-2, and 5 patients were classified as RCB-3.

## Clinical Outcomes

Based on RECIST, 11 (58%) of 19 patients achieved complete clinical response, that is, no palpable disease. This overestimates the true number of complete responders based on pathological examination. In the remaining 8 patients, 3 demonstrated a partial clinical response, 3 had stable disease, 1 had progressive disease, and 1 had missing clinical data before surgical resection.

## MBI T/B Ratio and Tumor Size Results

A summary of the absolute T/B ratio and change in T/B ratio at each time point is shown in Table 2. A trend of higher T/B ratio at baseline in the RCB-0 group compared with other groups was observed, but this association did not reach statistical significance. At 3 to 5 weeks, T/B ratio was lower in the RCB-0 group compared with the RCB-3 group (1.48 vs 2.36, $P = 0.043$). At post-NAC, T/B ratio of the RCB-0 group was lower than that of both the RCB-1/2 and RCB-3 groups (1.01 vs 1.3 [$P = 0.041$] and 1.01 vs 3.75 [$P = 0.002$], respectively).

Figure 1 shows the changes in T/B ratio over the 3 time points for each RCB group. The decrease in T/B ratio from baseline to 3 to 5 weeks was significantly greater for the RCB-0 group compared with the RCB-1/2 group (56% vs 28%, $P = 0.036$) and RCB-3 group (56% vs 4%, $P = 0.0001$). Likewise, the decrease in T/B ratio from baseline to post-NAC was significantly greater in the RCB-0 group compared with both RCB-1/2 (70% vs 55%, $P = 0.016$) and RCB-3 (70% vs −7%, P = 0.005) groups.

At 3 to 5 weeks, a trend in greater reduction in tumor size on MBI was noted in the RCB-0 group compared with RCB-1/2 and RCB-1/2 compared with RCB-3, but this association did

not reach statistical significance. After NAC, reductions in MBI-measured tumor size from baseline were nearly significant for the RCB-0 group compared with RCB-1/2 (100% vs 85%, $P = 0.055$) and significant for the RCB-0 group compared with the RCB-3 group (100% vs 20%, $P = 0.001$).

A difference in the pattern of change in tumor uptake was evident when the groups were divided by RCB classes (Fig. 1). The RCB-0 group showed a large initial drop in T/B ratio at 3 to 5 weeks, which contrasts sharply with the RCB-3 group, which showed minimal change in T/B ratio with NAC. In 2 of 5 women in the RCB-3 group, there was an increase in T/B ratio at 3 to 5 weeks. Figure 2 shows examples of MBI images at each of the time points for patients classified as RCB-0 and RCB-3.

Figure 3 illustrates the changes of T/B ratio from baseline to 3 to 5 weeks according to RCB groupings. The optimal threshold that gave the highest accuracy in discriminating between the RCB-1/2/3 and RCB-0 groups at 3 to 5 weeks was greater than 50% reduction in T/B ratio. Using this threshold to predict response, T/B ratio at 3 to 5 weeks demonstrated a diagnostic accuracy of 89.5% (95% CI, 0.64%–0.99%) in determining those in group RCB-0 versus those in groups RCB-1/2/3. The corresponding sensitivity and specificity were 92.3% (95% CI, 0.74%–0.99%) and 83.3% (95% CI, 0.44%–0.99%).

The 2 outliers in Figure 3 both demonstrated a marked change in the pattern of uptake between the 3- to 5-week and the final MBI studies. The first outlier was a patient who had estrogen receptor/progesterone receptor-positive, HER-2–negative infiltrating ductal carcinoma with extensive axillary disease at the time of diagnosis and was receiving sequential ACT (doxorubicin and cyclophosphamide followed by paclitaxel). There was an early 66% reduction of T/B ratio from baseline to 3 to 5 weeks but a 24% increase in T/B ratio from 3 to 5 weeks to completion of NAC. At surgery, she was found to have moderate residual disease (RCB-2).

The second outlier was a patient with triple negative infiltrating ductal carcinoma with axillary involvement who also received sequential ACT. At 3 to 5 weeks, T/B ratio demonstrated a poor response to NAC (17% reduction in uptake), but subsequently demonstrated a 59% reduction in T/B ratio between the last 2 MBI time points with no detectable disease on final MBI and no pathological evidence of residual disease at surgery (RCB-0). This may reflect a greater response to the second half of her chemotherapy, when she was switched from doxorubicin and cyclophosphamide to paclitaxel.

The AUC of the ROCs for reduction in T/B ratio at 3 to 5 weeks was 0.88, whereas the corresponding AUC for reduction in tumor size was 0.76 (Fig. 4). Post-NAC, the AUCs for T/B ratio and tumor size were 0.92 and 0.85, respectively. The correlation coefficient between MBI tumor size post-NAC and pathological tumor size was 0.95. All of the 8 patients with pCR had a corresponding post-NAC MBI study, which correctly demonstrated no abnormal uptake.

### MBI Comparison to Clinical Assessment and Other Tests

Seventeen of 19 patients had mammography and ultrasound performed post-NAC, and 18 of 19 patients had clinical examination performed post-NAC. In the 8 patients with pCR (no residual in-breast disease), post-NAC MBI was negative in all 8; post-NAC mammography was performed in 7 patients and negative in 6 of 7 patients; post-NAC ultrasound was negative in 2 of 8 patients, and clinical examination was negative in 6 of 8 patients.

Post-NAC MBI demonstrated better correlation with pathological size compared with correlations of post-NAC mammography (0.95 vs 0.79, $P = 0.0375$), ultrasound (0.95 vs

0.54, $P = 0.0008$), and clinical examination (0.95 vs 0.75, $P = 0.0168$) with pathological size.

## DISCUSSION

This study demonstrates that dedicated breast imaging with $^{99m}$Tc-sestamibi may have value in monitoring the response of tumors to NAC. A reduction in T/B ratio of greater than 50% demonstrated the ability to differentiate responders from nonresponders with an accuracy of 89.5% as early as 3 to 5 weeks after the initiation of NAC. These findings are similar to those of Mankoff et al,[15] who found a greater than 40% reduction in tumor uptake of $^{99m}$Tc-sestamibi after 8 weeks of NAC to be predictive of pathologic complete response. The use of a higher threshold in this study is most likely due to the better energy resolution of ~5% and consequently the lower scatter content of images acquired on the DC-MBI systems compared with conventional gamma cameras (energy resolution ~10%) or BSGI systems (energy resolution ~15%).[18]

The AUC for determining the presence or absence of residual disease using T/B ratio change at 3 to 5 weeks was 0.88. This is comparable to the value of 0.82 reported by Duch et al[12] using FDG-PET, using a greater than 40% reduction in SUV from baseline to midcycle NAC. Results from the ACRIN 6657 trial using changes in tumor size on MRI achieved an AUC of ~0.70.[27] In this study, changes in tumor size between responders and nonresponders were not significantly different at 3 to 5 weeks, but changes in T/B ratio were. These findings suggest that when using functional imaging, changes in tumor function may be more useful than changes in tumor size in the prediction of pathological residual disease.

An intriguing finding in this study is shown in Figure 1, where a number of patients exhibited unexpected changes in the pattern of uptake between the 3-to 5-week and the post-NAC images. In 4 cases, an initial reduction in uptake at 3 to 5 weeks was followed by a subsequent increase in uptake and a single case where the opposite pattern occurred. Four of these 5 patients had received sequential ACT. This was a 24-week regimen in which a doxorubicin/cyclophosphamide combination was administered before and separately from a taxane, which was introduced in the latter cycles. How breast cancer responds to NAC is complex and multifactorial. Breast cancer is not a single entity and consists of different molecular breast cancer subtypes (luminal A, luminal B, HER-2, triple negative, etc), all differing in terms of their response to a given chemotherapeutic agent.[28] It is likely that the response of these different subtypes will vary over time and may explain the change in response to change in the chemotherapeutic agents. Attempting to utilize a single time point in the treatment cycle to predict response may not be the ideal, and repeating the MBI shortly after switching to the second chemotherapeutic agent may be worth evaluating. A cost-effectiveness model reported by Schegerin et al[29] showed that even a small improvement in cure rate with NAC would generally outweigh the cost of prognostic imaging. Direct conversion–MBI is a relatively inexpensive imaging procedure (approximately 1.5 times that of digital mammography). Hence, more frequent imaging with DC-MBI during the course of NAC should both be cost-effective and enable better management of the disease.

There is a need to standardize response to NAC seen on functional imaging. Response classifications such as the RECIST, which are based on anatomic measurements of tumor size, are not well suited to functional imaging techniques such as MBI or PET/CT. We are not aware of any prior work on assessing changes in T/B ratio using dedicated gamma imaging of the breast; however, Tiling et al[16] showed an excellent correlation ($R = 0.86$) between tumor-to-lung ratio assessed with sestamibi and SUVmax and concluded that both FDG and sestamibi were equivalent for monitoring the response to NAC. With the reduced

scatter content of images acquired using DC-MBI, we would anticipate that this technology will enable more accurate and reproducible estimation of tumor uptake than previously possible with BSGI or conventional gamma camera systems.

One benefit of MBI compared with PET/CT derives from the behavior of the 2 radiopharmaceuticals used. $^{99m}$Tc-sestamibi has the advantage of rapid uptake in breast tissue with minimal redistribution over the first hour after injection.[20] By comparison, the uptake of FDG in tumors is dependent on blood glucose levels and increases with time, making it critical that FDG studies adhere to a consistent time interval between injection and imaging for reproducibility.

Estimation of tumor size post-NAC from MBI appears to correlate better with pathological tumor size than mammography, ultrasound, or clinical assessment. We have not compared estimation of tumor size from MBI with that from MRI, but would anticipate that it would be comparable in accuracy.

A limitation of MBI is its inability to depict axillary node involvement and potentially to visualize tumors close to the chest wall. Larger studies evaluating MBI in monitoring response to NAC are needed to confirm the findings reported here.

## CONCLUSIONS

In our study, quantitative assessment of tumor uptake of $^{99m}$Tc-sestamibi with a DC-MBI system demonstrated the ability to differentiate between pathological responders and nonresponders as early as 3 to 5 weeks after initiation of NAC. As a summary statistic for determining the presence or absence of residual disease, the AUC using differing thresholds of T/B ratio change at 3 to 5 weeks was 0.88. Taking a threshold of 50% reduction in T/B ratio at 3 to 5 weeks, MBI had an accuracy of 89.5% for predicting the presence or absence of residual disease at surgical resection. Early MBI at 3 to 5 weeks demonstrated statistically significant differences in the mean changes of T/B ratio between RCB groupings. Tumor size post-NAC from MBI correlated better with pathological tumor size than mammography, ultrasound, or clinical assessment. Our results are promising, but larger studies evaluating the use of $^{99m}$Tc-sestamibi and dedicated gamma cameras are needed to support these findings.

## Acknowledgments

Conflicts of interest and sources of funding: Mayo Foundation and 2 of the coinvestigators (M.K.O., C.B.H.) have a conflict of interest due to licensing arrangements between Mayo Foundation and Gamma Medica, a manufacturer of a direct conversion MBI system, for rights to the hardware and software technology developed for low-dose imaging. This conflict is noted in all the consent forms. This work was supported in part by the National Institutes of Health (grant CA128407).

## REFERENCES

1. Fisher B, Brown A, Mamounas E, et al. Effect of preoperative chemotherapy on local- regional disease in women with operable breast cancer: findings from National Surgical Adjuvant Breast and Bowel Project B-18. J Clin Oncol. 1997; 15:2483–2493. [PubMed: 9215816]
2. Fisher B, Bryant J, Wolmark N, et al. Effect of preoperative chemotherapy on the outcome of women with operable breast cancer. J Clin Oncol. 1998; 16:2672–2685. [PubMed: 9704717]
3. Gianni L, Baselga J, Eiermann W, et al. Phase III trial evaluating the addition of paclitaxel to doxorubicin followed by cyclophosphamide, methotrexate, and fluorouracil, as adjuvant or primary systemic therapy: European Cooperative Trial in Operable Breast Cancer. J Clin Oncol. 2009; 27:2474–2481. [PubMed: 19332727]

4. Mamounas EP, Brown A, Anderson S, et al. Sentinel node biopsy after neoadjuvant chemotherapy in breast cancer: results from National Surgical Adjuvant Breast and Bowel Project Protocol B-27. J Clin Oncol. 2005; 23:2694–2702. published correction appears in J Clin Oncol 2005;23:2694-2702. [PubMed: 15837984]
5. Bear HD, Anderson S, Brown A, et al. The effect on tumor response of adding sequential preoperative docetaxel to pre-operative doxorubicin and cyclo-phosphamide: preliminary results from National Surgical Adjuvant Breast and Bowel Project Protocol B-27. J Clin Oncol. 2003; 21:4165–4174. [PubMed: 14559892]
6. Hunt KK, Yi M, Mittendorf EA, et al. Sentinel lymph node surgery after neoadjuvant chemotherapy is accurate and reduces the need for axillary dissection in breast cancer patients. Ann Surg. 2009; 250:558–566. [PubMed: 19730235]
7. Bear HD, Tang G, Rastogi P, et al. Bevacizumab added to neoadjuvant chemotherapy for breast cancer. N Engl J Med. 2012; 366:310–320. [PubMed: 22276821]
8. Barker AD, Sigman CC, Kelloff GJ, et al. I-SPY 2: an adaptive breast cancer trial design in the setting of neoadjuvant chemotherapy. Clin Pharmacol Ther. 2009; 86:97–100. [PubMed: 19440188]
9. Food and Drug Administration. Guidance for Industry Pathologic Complete Response in Neoadjuvant Treatment of High-Risk Early-Stage Breast Cancer: Use as an Endpoint to Support Accelerated Approval. US Department of Health and Human Services; 2012. Available at: http://www.fda.gov/downloads/Drugs/GuidanceComplianceRegulatoryInformation/Guidances/UCM305501.pdf [Accessed October 1, 2013]
10. Chagar AB, Middleton LP, Sahin AA, et al. Accuracy of physical examination, ultrasonography, and mammography in predicting residual pathologic tumor size in patients treated with neoadjuvant chemotherapy. Ann Surg. 2006; 243:257–264. [PubMed: 16432360]
11. Prevos R, Smidt ML, Tjan-Heijnen VCG. Pre-treatment differences and early response monitoring of neoadjuvant chemotherapy in breast cancer patients using magnetic resonance imaging: a systematic review. Eur Radiol. 2012; 22:2607–2616. [PubMed: 22983282]
12. Duch J, Fuster D, Montserrat M, et al. $^{18}$F-FDG PET/CT for early prediction of response to neoadjuvant chemotherapy in breast cancer. Eur J Nucl Med Mol Imaging. 2009; 36:1551–1557. [PubMed: 19326117]
13. Koolen BB, Vrancken Peeters MJ, Wesseling J, et al. Association of primary tumour FDG uptake with clinical, histopathological and molecular characteristics in breast cancer patients scheduled for neoadjuvant chemotherapy. Eur J Nucl Med Mol Imaging. 2012; 39:1830–1838. [PubMed: 22895862]
14. Groheux D, Giacchetti S, Espie M, et al. Early monitoring of response to neoadjuvant chemotherapy in breast cancer with $^{18}$F-FDG PET/CT: defining a clinical aim (Editorial). Eur J Nucl Med Mol Imaging. 2011; 38:419–425. [PubMed: 21072510]
15. Mankoff DA, Dunwald LK, Gralow JR, et al. Monitoring the response of patients with locally advanced breast carcinoma to neoadjuvant chemotherapy using [technetium 99m]-sestamibi mammoscintigraphy. Cancer. 1999; 85:2410–2423. [PubMed: 10357412]
16. Tiling R, Linke R, Untch M, et al. $^{18}$F-FDG PET and 99mTc-sestamibi scintimammography for monitoring breast cancer response to neoadjuvant chemotherapy: a comparative study. J Nucl Med. 2001; 28:711–720.
17. Brem RF, Rapelyea JA, Zisman G, et al. Occult breast cancer: scintimammography with high resolution breast-specific gamma camera in women at high risk for breast cancer. Radiology. 2005; 237:274–280. [PubMed: 16126919]
18. Hruska CB, O'Connor MK, Collins DA. Comparison of small field of view gamma camera systems for scintimammography. Nucl Med Commun. 2005; 26:441–445. [PubMed: 15838427]
19. O'Connor MK, Waganeer DJ, Hruska CB, et al. Molecular Breast Imaging using a dedicated high-performance instrument. Proceeding of SPIE. 2006; 6319:63191D1–63191D14.
20. Hruska CB, Weinmann AL, Tello-Skjerseth CM, et al. Proof of concept for low-dose molecular breast imaging with a dual-head CZT gamma camera. Part II. Evaluation in patients. Med Phys. 2012; 39:3476–3483. [PubMed: 22755727]

21. Hruska CB, Phillips SW, Whaley DH, et al. Molecular breast imaging: use of a dual-head dedicated gamma camera to detect small breast tumors. Am J Roentgenol. 2008; 191:1805–1815. [PubMed: 19020253]
22. O'Connor MK, Phillips SW, Hruska CB, et al. Molecular breast imaging: advantages and limitations of a scintimammographic technique in patients with small breast tumors. Breast J. 2007; 13:3–11. [PubMed: 17214787]
23. Gunasekera RD, Notghi A, Mostafa AB, et al. Adsorption of radiopharmaceuticals to syringes leads to lower administered activity than intended. Nucl Med Commun. 2001; 22:493–497. [PubMed: 11388569]
24. Conners AL, Hruska CB, Tortorelli CL, et al. Lexicon for standardized interpretation of gamma camera molecular breast imaging: observer agreement and diagnostic accuracy. Eur J Nucl Med Mol Imaging. 2012; 39:971–982. [PubMed: 22289959]
25. Symmans WF, Peintinger F, Hatzis C, et al. measurement of residual breast cancer burden to predict survival after neoadjuvant chemotherapy. J Clin Oncol. 2007; 25:4414–4422. [PubMed: 17785706]
26. Eisenhauer EA, Therasse P, Bogaerts J, et al. New response evaluation criteria in solid tumours: revised RECIST guideline (version 1.1). Eur J Cancer. 2009; 45:228–247. [PubMed: 19097774]
27. Hylon NM, Blume JD, Bernreuter WK, et al. Locally advanced breast cancer: MR imaging for prediction of response to neoadjuvant chemotherapy–results from ACRIN 6657/I-SPY trial. Radiology. 2012; 265:663–672.
28. Perou CM, Sørlie T, Eisen MB, et al. Molecular portraits of human breast tumours. Nature. 2000; 406:747–752. [PubMed: 10963602]
29. Schegerin M, Tosteson ANA, Kaufman PA, et al. Prognostic imaging in neoadjuvant chemotherapy of locally advanced breast cancer should be cost-effective. Breast Cancer Res Treat. 2009; 114:537–547. [PubMed: 18437559]

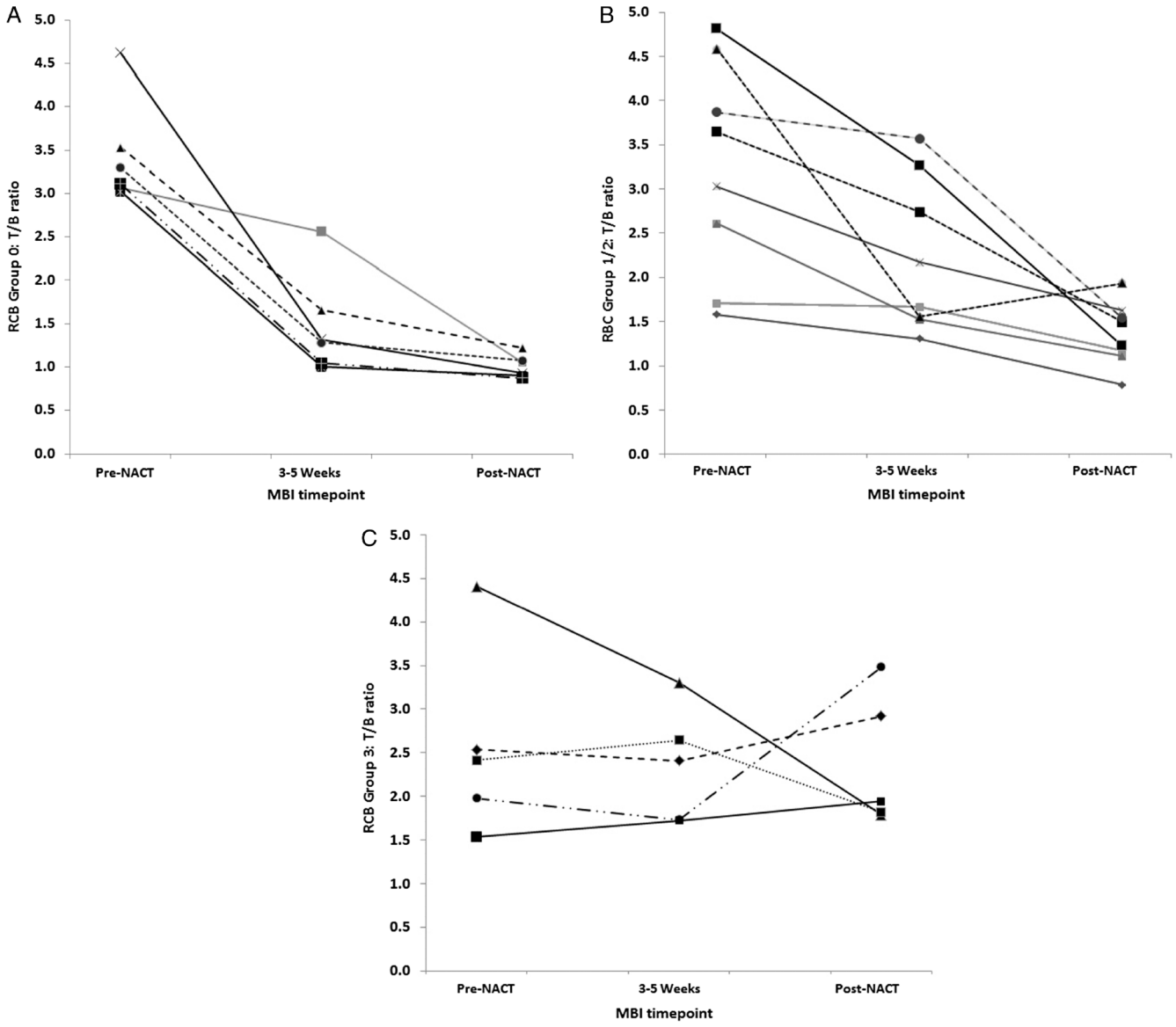


**FIGURE 1.**

Tumor-to-background ratio obtained at baseline, 3 to 5 weeks into NAC, and post-NAC for the 19 patients in (A) RCB-0, (B) RCB-1/2, and (C) RCB-3 groups.

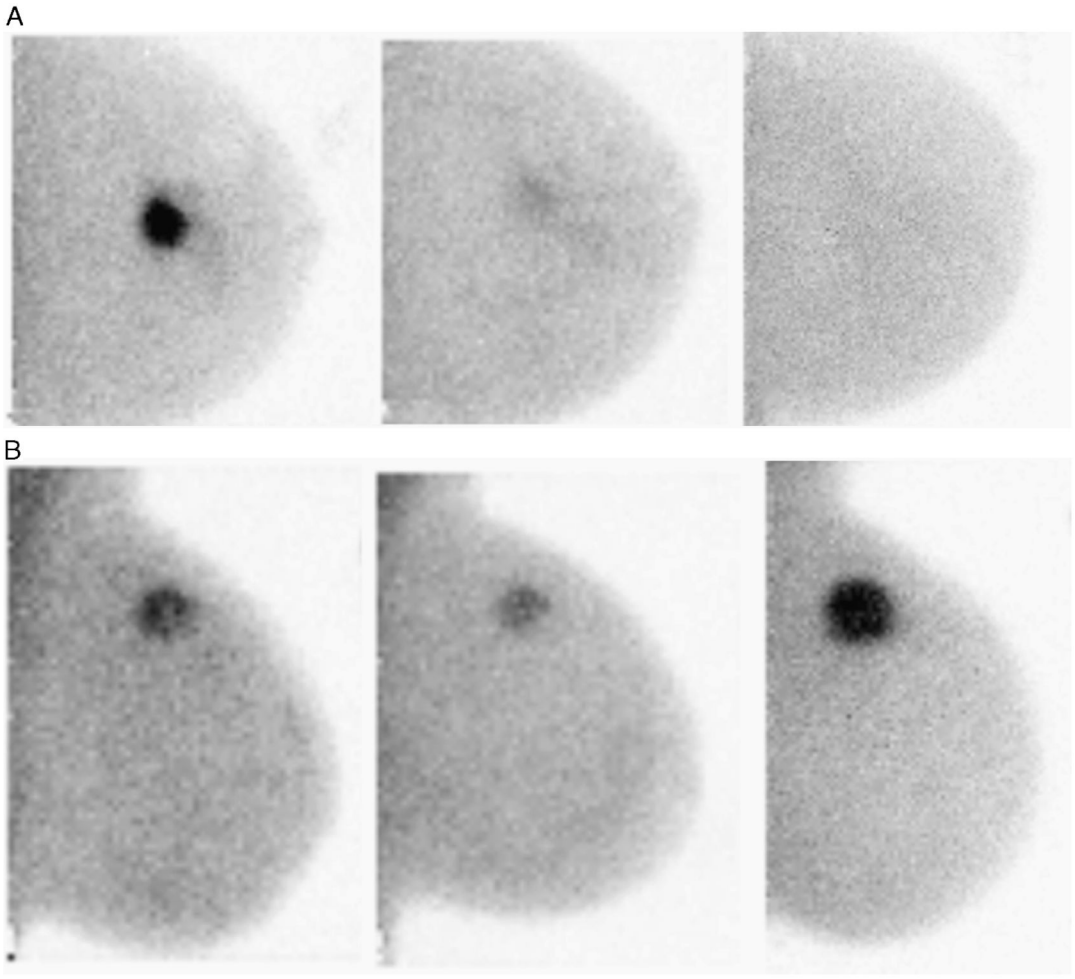


**FIGURE 2.**
Molecular breast imaging images acquired pre-NAC, at 3 to 5 weeks and after completion of NAC. A, Left CC MBI images in a patient classified as a responder (RCB-0). B, left MLO MBI images in a patient classified as a nonresponder (RCB-3). Note the relative increase in uptake from the second to the third image.

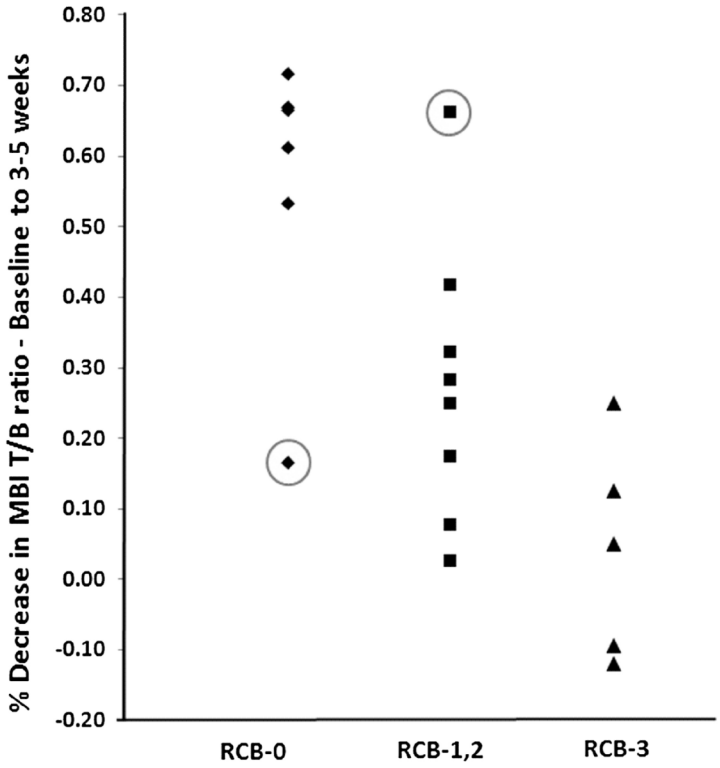


**FIGURE 3.**
Percent changes in the MBI T/B ratio from baseline to 3 to 5 weeks for the 19 patients divided into RCB groupings. The 2 outliers in RCB-0 and RCB-1, RCB-2 are circled.

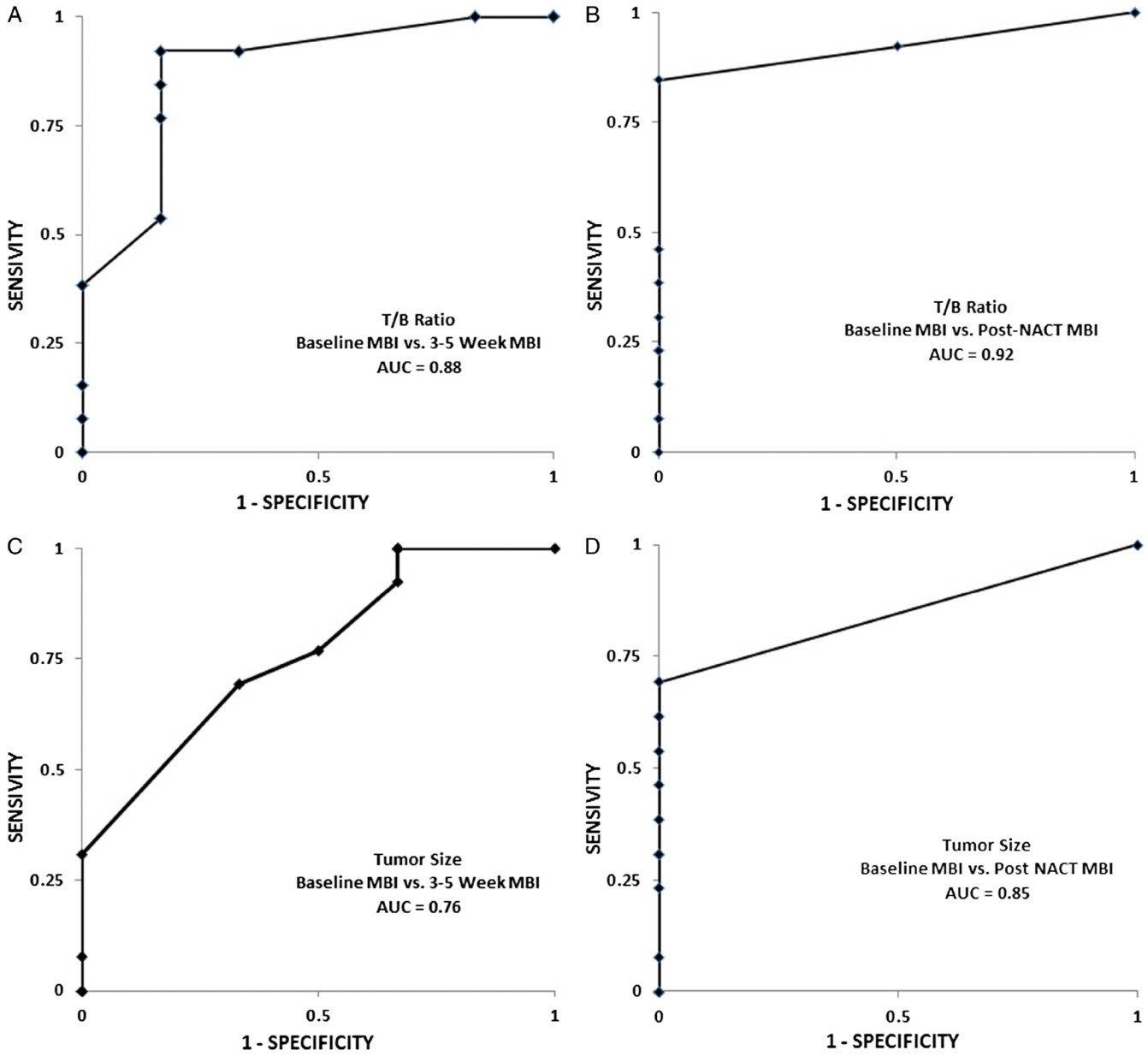


**FIGURE 4.**

Receiver operator characteristic curves for distinguishing patients with RCB category RCB-0 from RCB-1/2/3 groups using the T/B ratio from the (A) 3- to 5-week and (B) post-NAC MBI studies. Comparable curves are shown using tumor size ratio from the (C) 3- to 5-week and (D) post-NAC MBI studies.

## TABLE 1

Characteristics of 19 Study Participants Who Underwent NAC for Breast Cancer

| Characteristics | Characteristic Subtype | Value |
|---|---|---|
| Age | Median (Range) 48 | (36–73) |
| | Mean (SD) | 49.7 (9.9) |
| Race or ethnicity | White | 18 (95%) |
| | Black or African American | 1 (5%) |
| | Hispanic or Latina | 0 |
| | Asian | 0 |
| | Other | 0 |
| | Unknown | 0 |
| Menopausal status | Premenopausal | 8 (42%) |
| | Perimenopausal | 4 (21%) |
| | Postmenopausal | 7 (37%) |
| BI-RADS breast density category | Entirely fat | 0 |
| | Scattered fibroglandular densities | 11 (58%) |
| | Heterogeneously dense | 7 (37%) |
| | Extremely dense | 1 (5%) |
| Receptor status | Hormone receptor positive/ HER-2 negative | 9 (47%) |
| | HER-2 positive | 4 (21%) |
| | Triple negative (ER/PR/HER-2 negative) | 6 (32%) |
| Tumor histology | Invasive ductal carcinoma | 17 (89%) |
| | Invasive lobular carcinoma | 0 |
| | Mixed invasive ductal/lobular carcinoma | 2 (11%) |
| Inflammatory breast cancer | | 2 (11%) |
| Multifocal/multicentric disease | | 4 (21%) |
| Contralateral/bilateral breast cancer | | 0 |
| Tumor size, pretreatment (clinical), mm | Median (Range) | 40 (0–80) |
| | Mean (SD) | 39.2 (21.3) |
| Tumor size, pretreatment (MRI) | Median (Range) | 37 (22–98) |
| | Mean (SD) | 42.5 (19.3) |
| Lymph node status at diagnosis | Positive | 10 (53%) |
| | Negative | 9 (47%) |
| Metastatic status at diagnosis | Distant metastasis | 0 |
| Neoadjuvant therapy | Doxorubicin/cyclophosphamide/ Paclitaxel | 7 (37%) |

| Characteristics | Characteristic Subtype | Value |
|---|---|---|
| | Carboplatin/paclitaxel | 7 (37%) |
| | Doxorubicin/cyclophosphamide | 2 (11%) |
| | Paclitaxel alone | 2 (11%) |
| | 5-Fluorouracil/epirubicin/ cyclophosphamide | 1 (5%) |
| Hormonal/biotherapy | Trastuzumab | 4 (21%) |
| | Hormonal therapy | 0 |
| Surgical treatment | Lumpectomy | 5 (26%) |
| | Unilateral mastectomy | 2 (11%) |
| | Bilateral mastectomy | 12 (63%) |
| Clinical response | Clinical complete response | 11 (58%) |
| | Partial response | 3 (16%) |
| | Stable disease | 3 (16%) |
| | Progressive disease | 1 (5%) |
| | Missing data | 1 (5%) |
| Pathological response in the breast | Complete response | 8 (42%) |
| | Residual invasive disease | 11 (58%) |
| RCB class | RCB-0 | 6 (32%) |
| | RCB-1 | 3 (16%) |
| | RCB-2 | 5 (26%) |
| | RCB-3 | 5 (26%) |

BI-RADS indicates Breast Imaging-Reporting and Data System; HER-2, Human Epidermal Growth Factor Receptor 2; ER/PR, estrogen receptor/ progesterone receptor.

## TABLE 2

Mean T/B Ratios and Tumor Size Measured by MBI Compared With Pathological Tumor Response

| Tumor/Background Uptake Ratio Category | Subcategory | RCB-0 | RCB-1/2 | RCB-3 |
|---|---|---|---|---|
| Baseline MBI T/B ratio | Mean T/B ratio (95% CI) | 3.44 (2.95–3.93) | 2.98 (2.02–3.94) | 2.58 (1.70–3.46) |
| | Comparison to RCB-0 (*P*) | | 0.705 | 0.131 |
| 3- to 5-wk MBI T/B ratio | Mean T/B ratio (95% CI) | 1.48 (1.02–1.94) | 2.08 (1.38–2.78) | 2.36 (2.07–2.65) |
| | Comparison to RCB-0 (*P*) | | 0.093 | 0.043 |
| Post-NAC MBI T/B ratio | Mean T/B ratio (95% CI) | 1.01 (0.91–1.11) | 1.3 (1.01–1.59) | 3.75 (3.13–4.37) |
| | Comparison to RCB-0 (*P*) | | 0.041 | 0.002 |
| Baseline vs 3- to 5-wk MBI T/B ratio | Mean % decrease (95% CI) | 0.56 (0.40–0.72) | 0.28 (0.13–0.43) | 0.04 (−0.08–0.16) |
| | Comparison to RCB-0 (*P*) | | 0.036 | 0.001 |
| Baseline vs post-NAC MBI T/B ratio | Mean % decrease (95% CI) | 0.7 (0.66–0.74) | 0.55 (0.45–0.65) | −0.07 (−0.48–0.34) |
| | Comparison to RCB-0 (*P*) | | 0.016 | 0.005 |

| Tumor Size Category | Subcategory | RCB-0 | RCB-1/2 | RCB-3 |
|---|---|---|---|---|
| Baseline MBI size | Mean size (95% CI), cm | 3.82 (2.28–5.36) | 5.15 (3.09–7.21) | 4.64 (3.06–6.22) |
| | Comparison to RCB-0 (*P*) | | 0.308 | 0.502 |
| 3- to 5-wk MBI size | Mean size (95% CI), cm | 2.05 (0.47–3.63) | 3.4 (1.86–4.94) | 3.82 (2.53–5.11) |
| | Comparison to RCB-0 (*P*) | | 0.223 | 0.143 |
| Post-NAC MBI size | Mean size (95% CI), cm | 0 (0) | 0.74 (0–1.48) | 3.78 (2.39–5.17) |
| | Comparison to RCB-0 (*P*) | | 0.077 | <0.001 |
| Baseline vs 3- to 5-wk MBI size | Mean % decrease (95% CI) | 0.53 (0.23–0.83) | 0.35 (0.25–0.45) | 0.18 (0.11–0.25) |
| | Comparison to RCB-0 (*P*) | | 0.223 | 0.69 |
| Baseline vs post-NAC MBI size | Mean % decrease (95% CI) | 1 (1) | 0.85 (0.71–0.99) | 0.2 (0.09–0.31) |
| | Comparison to RCB-0 (*P*) | | 0.055 | <0.001 |